Chemisorption of NO_2 on Carbon Nanotubes

Wai-Leung Yim,[†] X. G. Gong,[†,‡,§] and Zhi-Feng Liu*[,†]

Department of Chemistry, The Chinese University of Hong Kong, Shatin, Hong Kong, China; Institute of Solid State Physics, Chinese Academy of Sciences, Hefei, Anhui, China; and Surface Physics Laboratory and Department of Physics, Fudan University, 200433−Shanghai, China

Received: December 7, 2002; In Final Form: June 2, 2003

The chemisorption of NO_2 on carbon nanotubes is studied by modeling the interaction between NO_2 and N_2O_4 with an infinitely long (8,0) single-walled carbon nanotube, using planewave/pseudopotential-based density functional theory (DFT). In sharp contrast to the case of graphite, for which NO_2 adsorption is physical, a NO_2 radical could readily adsorb on the exterior of an (8,0) tube by addition, similar to the reaction between NO_2 and alkenes. The process is slightly endothermic and reversible with a low energy barrier, with the NO_2 group in either the nitro or nitrite configuration. Adsorption of a second NO_2 is considerably exothermic, and desorption of NO_2 from such a configuration is much more difficult. The chemisorption of NO_2 also increases the conductivity of the (8,0) tube. On the other hand, N_2O_4 only plays a minor role in the equilibrium between desorption and adsorption processes. These results indicate that the (8,0) tube is more reactive toward NO_2 than graphite, due to the curvature on the rolled graphene sheet.

Introduction

It is well-known that a graphene sheet is chemically inert, due to the extensive conjugate π bonding among the carbon atoms on the 2D lattice. Rolling up graphene sheets produces carbon nanotubes,[1] a new class of materials that have attracted much attention in the past few years for their potential applications as nanodevices.[2] With a curvature in the graphene sheet, the conjugate π bond should be less effective on the wall of a carbon nanotube than that on a flat graphene sheet, and there is hybridization between the π and σ orbitals. It is interesting to ask whether such changes in bonding would make carbon nanotubes chemically more reactive.

Understanding such changes is important for the study of gas adsorption on carbon nanotubes, a topic that has generated much interest in recent studies. It was observed that carbon nanotubes could take up a large amount of hydrogen gas, making it a potential medium for hydrogen storage.[3−5] Hydrogen adsorption on the wall of a carbon nanotube should be physical,[6,7] but such interactions cannot yet account for the experimentally observed hydrogen storage.[8] It is possible for a H_2 molecule to undergo concerted dissociative adsorption in a bundle of carbon nanotubes, by depositing each hydrogen atom on one of the two adjacent tubes, although the process could only take place under high pressure and high temperature.[9]

Electric and thermal conductance of carbon nanotubes was found to be very sensitive to oxygen exposure.[10,11] O_2 reacts readily with the edges or caps of carbon nanotubes and with fullerenes.[12] But on the tube wall, the interaction is again found to be dominated by physisorption,[12,13] with chemisorption playing a very minor role.[14,15] On the other hand, chemisorption of ozone on tube walls has been established by both experiments[16,17] and theoretical calculations.[18]

The change of physical properties after gas exposure implies the application of carbon nanotubes as chemical sensors. This idea was first explored by Kong and co-workers[19] for NO_2 and NH_3. Significant changes in electric resistance were picked up within minutes after gas exposure, making carbon nanotubes potentially very sensitive detectors for these toxic gases. In addition, these carbon nanotubes can be recovered after desorption, although the process took much longer (∼12 h) than adsorption. The interaction between NO_2 and the walls of carbon nanotubes was found to be dominated by physisorption, based on density functional theory (DFT) calculations.[20−22]

NO_2 is known as a reactive gas, especially with water, and also as a pollutant in the atmosphere.[23] As a radical, it reacts with alkenes at room temperature,[24−26] producing a wide variety of hazardous pollutants in the atmosphere. Such reactions could be initiated either by a hydrogen abstraction mechanism, in which the NO_2 radical takes a hydrogen atom from an alkene,[28,29] or, more relevant to our study on carbon nanotubes, by direct addition to a C═C double bond to produce an organic radical.[30−32] On the other hand, it has been well established experimentally that the NO_2 adsorption on graphite is physical, with a weak interaction energy.[33,34] On a flat graphene sheet, formation of a σ N−C bond with tetrahedron geometry around the C atom is not favored, due to the well-known stabilization effect by the extensive conjugate π bonding among carbon atoms. This is probably the reason only physisorption is considered in the previous studies on the interaction between NO_2 and carbon nanotubes.[20−22]

However, the reaction with NO_2 is actually an interesting test of the reactivity of carbon nanotubes. As a graphene sheet is rolled up to produce a single-walled carbon nanotube, is it still chemically as inert as a graphene? Or is the tension on the curved surface strong enough to make it similar to an alkene and vulnerable to addition by the NO_2 radical? In this paper, we report DFT calculations on the chemisorption of both NO_2 and N_2O_4 on the wall of an infinitely long (8,0) carbon nanotube, with a careful examination of a number of configurations. The calculated energetics and reaction barriers indicate that chemisorption takes place readily, providing an example for the enhanced reactivity of carbon nanotube walls, in contrast to graphite.

* Corresponding author.
[†] The Chinese University of Hong Kong.
[‡] Chinese Academy of Sciences.
[§] Fudan University.

10.1021/jp027647l CCC: $25.00
Published on Web 07/29/2003

Computational Methods

The interaction between NO_2 and an (8,0) carbon nanotube is studied by density functional theory with a plane wave basis set and pseudopotentials for the atomic core regions,[35−37] as implemented within the Vienna ab initio simulation package (VASP).[38−41] This method has been applied to a variety of chemical problems in recent years.[42,43] A plane wave basis set with a cutoff energy of 270.2 eV is used for the electron wave function, which is solved by residual minimization of the total electronic energy. The local density approximation (LDA)[44] is used to study some of the physisorption configurations, so that they could be compared with previous LDA results. But for the calculation of energetics and structures involved in chemisorption, the PW91[45] gradient correction is added to the exchange-correlation functional. For the core region, the optimized Vanderbilt ultrasoft pseudopotentials[46] supplied with the VASP[47,48] are directly used for the C, N, and O atoms. Two k-points generated by the Monkhorst−Pack method[49] are used in the k-space sampling. Similar setups have been tested before for the adsorption of H_2 and O_2 on carbon nanotubes.[9,14]

An infinitely long (8,0) single-walled carbon nanotube is modeled by a periodic box. The lattice parameters *a* and *b* at 15 Å are large enough so that the interaction between tubes in neighboring cells is negligible, while *c* at 8.61 Å is adjusted to the periodicity along the tube. When NO_2 is present, spin-polarized density (open shell) is used, while, for the adsorption of N_2O_4, spin-restricted density (close shell) is used to reduce computational cost.

The geometry was optimized by conjugate gradient minimization of the total energy versus the atomic coordinates. The minimum energy reaction path is mapped out first by the nudged elastic band method,[50−52] while the transition structure is further refined by the CLIMBING method,[53,54] both developed by Jónsson and co-workers.

Results and Discussions

1. Overview. For a complete understanding of NO_2 adsorption on the exterior of a carbon nanotube, three factors must be taken into consideration. The first is the orientation of the triangular shaped NO_2 relative to the nanotube surface, as schematically illustrated in Figure 1. In the nitro configuration, the NO_2 molecule is bonded to the tube surface with the nitrogen end. Bonding with one oxygen end produces the nitrite configuration, while bonding with both oxygen ends produces the cycloaddition configuration. These configurations are important for both physisorption and chemisorption.

In previous studies on physisorption, only the nitro configuration was considered,[20,21] and the binding energy was found to be 0.42 eV (9.7 kcal/mol) at the LDA level.[21] The value was compared to the experimentally determined physisorption energy of 0.4 eV (9.2 kcal/mol) on a graphite surface,[33] which was actually for N_2O_4. In good agreement with these results, our calculations at the LDA level found a binding energy of 8.0 kcal/mol for the physisorbed nitro configuration, with the energy defined for both physisorption and chemisorption, shown in Figure 2, as

$$\Delta E = E(\text{adsorption structure}) - E(\text{bare tube}) - E(NO_2)$$

As shown in Table 1, other physisorption configurations are also found in our calculations, and the adsorption energy varies slightly. When gradient correction is added at the PW91 level, the calculated adsorption energy decreases to the range 3−5 kcal/mol, as it is well-known that binding energy is often overestimated at the LDA level. Adsorption with the oxygen end produces slightly higher binding energy, which could be attributed to the fact that the oxygen atoms are electron rich in the NO_2 molecule.

The second factor is the presence of multiple adsorption sites along the exterior of a carbon nanotube, and the possibility of

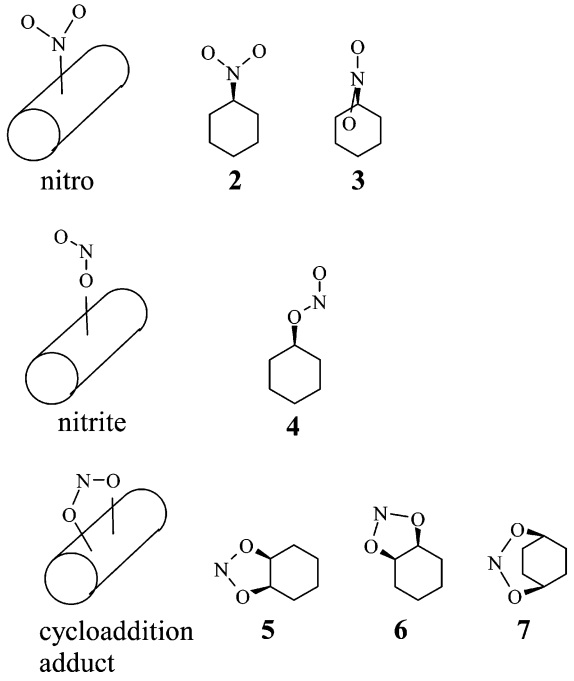

Figure 1. Possible configurations for physisorption and chemisorption of one NO_2 group on the exterior of a carbon nanotube.

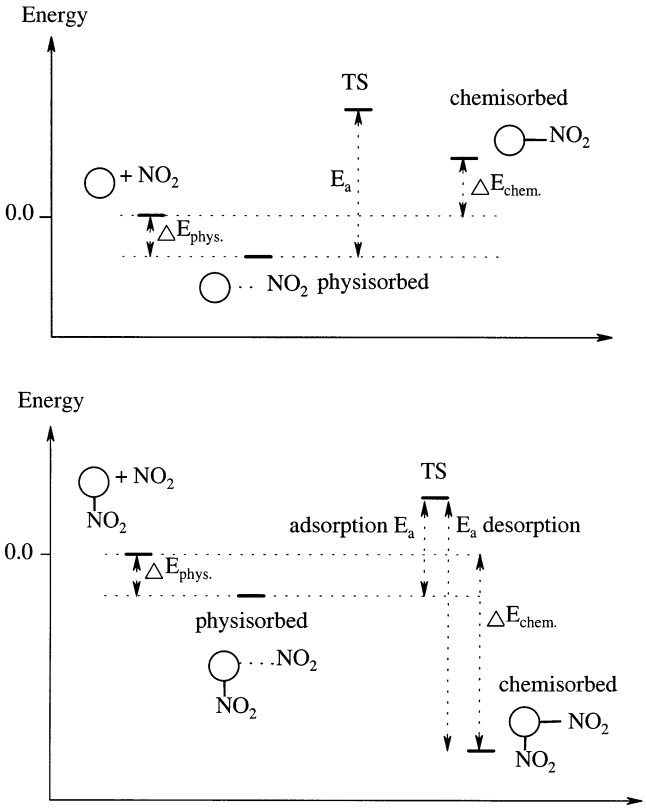

Figure 2. Schematics for the chemisorption of one and two NO_2 groups on an (8,0) tube. The first chemisorption, shown at the top, is slightly endothermic, with a low barrier, while the second chemisorption, shown at the bottom, is exothermic, again with a low reaction barrier. For the actual values, see Tables 1 and 2.

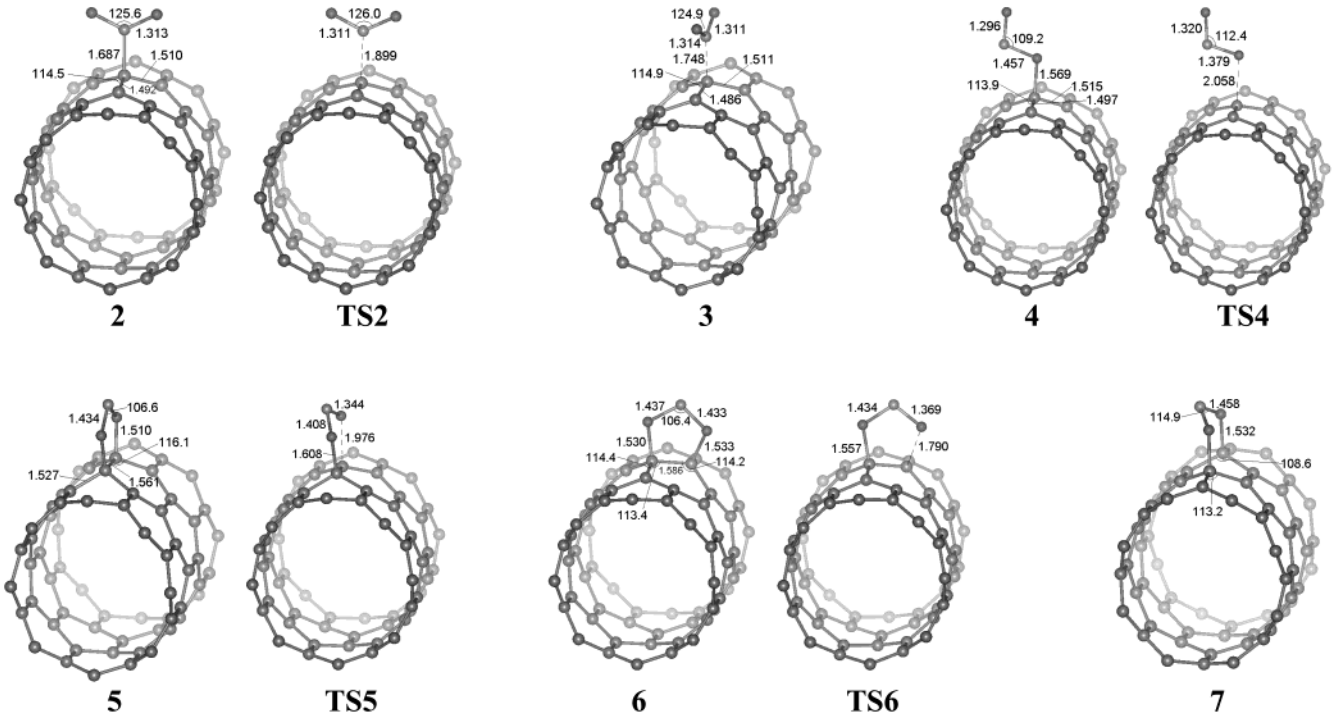

Figure 3. Optimized structures and transition structures for the adsorption of one NO_2 group on an (8,0) single-walled carbon nanotube. The distances shown are in angstroms.

TABLE 1: Energetics[a] for the Physisorption and Chemisorption of One NO_2 Group on an (8,0) Carbon Nanotube, with Energy in kilocalories per mole

	LDA	GGA		
structure	ΔE_{phys}	ΔE_{phys}	ΔE_{chem}	E_a (chemisorption barrier)
2	−9.1	−3.9	1.5	5.7
3	−7.5	−3.3	4.4	7.7[b]
4	−5.9	−4.2	1.3	9.4
5	−9.6	−4.8	1.3	14.2
6	−9.0	−4.4	11.5	17.9
7	−9.0	−4.6	30.4	35.0[b]

[a] The energetics is defined in Figure 2. [b] In these two cases, the total energy increases monotonically from the physisorption to the chemisorption structure along the reaction path, and no transition state is identified.

multiple adsorption. The adsorption of two NO_2 groups is especially important, as it saturates the two radicals. Finally, the NO_2 gas under ambient conditions is a textbook example of chemical equilibrium, between NO_2 and N_2O_4. For a complete analysis, the interaction between the carbon nanotube and both NO_2 and N_2O_4 must be understood, so that the adsorption and desorption processes can be considered together with the equilibrium between NO_2 and N_2O_4.

2. Chemisorption of a Single NO_2. In terms of chemical bonding, the chemisorption with a nitro configuration (**2** in Figure 3) is the most straightforward, with the formation of a C−N bond. The energy barrier for this process is only 5.7 kcal/mol. However, the overall chemisorption process is endothermic, although by only 1.5 kcal/mol (Table 1). This is contrary to the usual situation, in which the binding energy for chemisorption should be much larger than that for the physisorption. As a C−N bond is formed in **2**, the carbon atom is pulled up slightly from the cylindrical nanotube surface. Two of the NCC angles are 107.4°, while the third (with C−C along the tube) is 103.3°. For the CCC angles, two are 114.5°, while the third is 109.0°. The weak C−N bond can be attributed to the deviation from the ideal tetrahedron angle of 109.5° for some of the bond angles. The weak C−N bond is also reflected in its distance of 1.69 Å, compared to the typical C−N distance of 1.5 Å. Nonetheless, with the graphene sheet rolled up, chemisorption of NO_2 on a (8,0) carbon nanotube is now possible, although the process is thermally almost neutral. The NO_2 group in **2** could also rotate along the C−N bond as in **3**, and when the two oxygen atoms are along the tube direction, the energy is raised by 2.9 kcal/mol.

For the nitrite **4** and the cycloaddition **5**, the chemisorption process is again only slightly endothermic. However, there is an appreciable rise in the energy barrier for the chemisorption processes leading to these two structures. It could be attributed to the fact that these processes involve the rearrangement for the N−O bonds in the NO_2 group, which raises the reaction barrier. The significant energy difference between **5** and **6** is also quite interesting, although both are ortho-cycloaddition products. The difference must be due to the orientation in regarding to the tube axis. For **5**, the saturated C═C bond is along the tube direction, while, for **6**, the C═C is along the circumference. We have also tried to find meta and para cycloaddition products, but they are considerably higher in energy.

On the basis of these results, NO_2 gas should readily chemisorb on the wall of an (8,0) carbon nanotube, as shown in Figure 2, especially in the nitro configuration. The process is reversible, similar to the addition of NO_2 to alkenes,[30,31] as the barriers for both adsorption and desorption are low. Among the possible configurations, the nitro (**2**) and nitrite (**4**) are the more important ones. Even though the process is slightly endothermic, the energy loss is quite small, and a chemical equilibrium is easily achieved in ambient conditions. Experimentally, a fast response in the conductivity of carbon nanotubes was observed after NO_2 exposure.[19]

3. Chemisorption of Two NO_2 Groups. With each carbon atom on the carbon nanotubes being a potential chemisorption site, the probability for multiple adsorption must be carefully considered. This is especially true after the chemisorption of the first NO_2 group in **2** and **4**, as the system now contains an

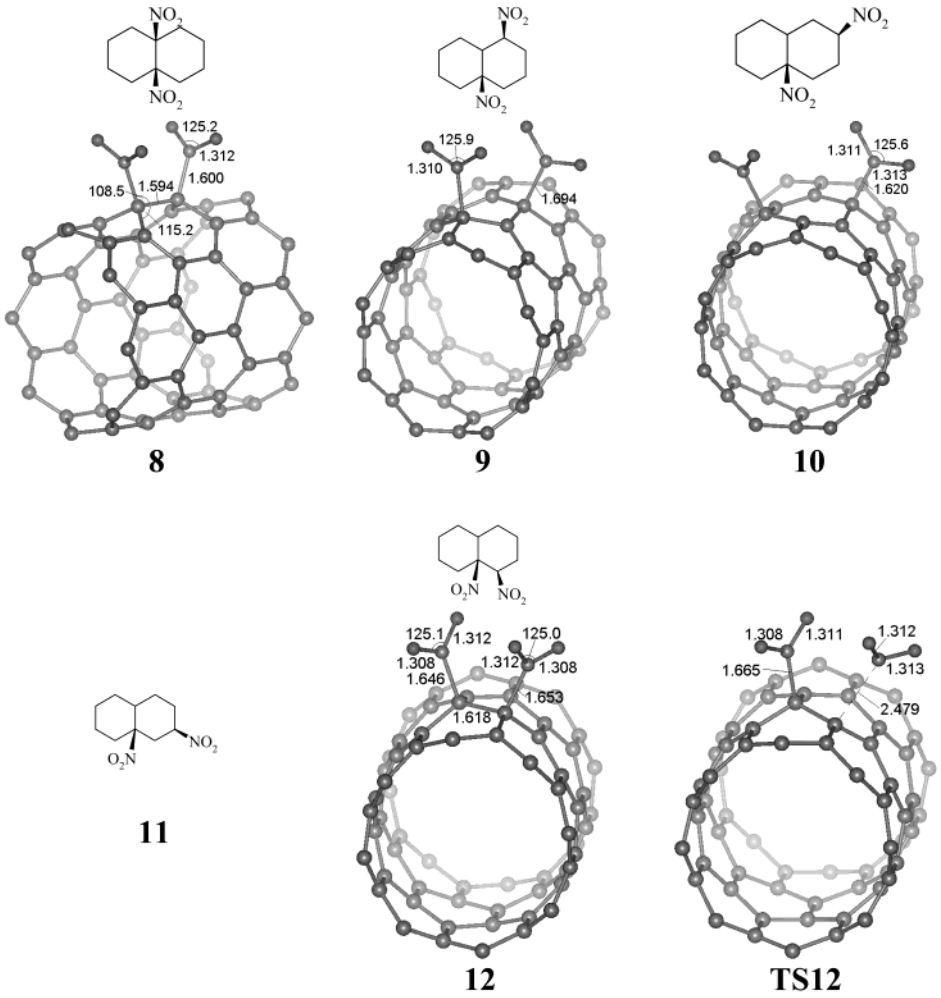

Figure 4. Optimized structures and transition structures for the adsorption of the second NO_2 on an (8,0) single-walled carbon nanotube in the nitro configuration. The distances shown are in angstroms.

unpaired electron, which could be paired up with the adsorption of a second NO_2.

Shown in Figure 4 are the five distinctive sites when the chemisorption of the second NO_2 group occurs on the same six-member carbon ring as the first NO_2. Although the unpaired electron on the nanotube wall introduced by the adsorption of NO_2 should be delocalized, it is nonetheless reasonable to assume that it is near the first adsorption site, and we only consider the sites in the same six-member ring with the first site. Also, as the nanotube is rolled up, the two ortho (or meta) positions are not equivalent to each other. Similarly, the doubly adsorbed NO_2 groups in nitrite configurations are shown in Figure 5.

In terms of energy, chemisorption of the second NO_2 is exothermic for the ortho and para positions. As shown in Table 2, the most favorable cases are −15.3 kcal/mol for the nitro configuration (**8** in Figure 4) and −21.4 kcal/mol for the nitrite configuration (**13** in Figure 5). On the other hand, the meta configurations are either unstable (**9** for the nitro configurations in Figure 4) or endothermic (**14** and **16** for the nitrite configurations in Figure 5). Furthermore, we were unable to locate a stable structure for the meta configuration **11**. Such observations can be explained by considering the resonance structures after the addition of the first NO_2 group, which favors structures with the unpaired electron at either the ortho or para position.[55]

The nitro and nitrite configurations differ from each other in two aspects. As far as energy is concerned, the nitrite configurations are more stable than their corresponding nitro configurations, which is consistent with previous calculations on other systems.[56] On the other hand, the reaction barrier for nitrite adsorption is also higher than that for the nitro configurations, for which there is almost no barrier. This is similar to the situation in the first NO_2 adsorption and can be attributed again to the rearrangement in the N−O bond during the nitrite adsorption.

The energy difference between the two ortho configurations **8** and **12** is an interesting illustration of the special bonding environment on the carbon nanotube surface. Part of it could be attributed to the orientation of the NO_2 group. As discussed previously for the single nitro chemisorption structures **2** and **3**, the NO_2 group prefers an orientation with the NO_2 plane perpendicular to the tube axis. In **8**, the saturated C−C bond lies along the tube, and the NO_2 planes maintain their orientation perpendicular to the tube axis. In contrast, for **12**, the saturated C−C bond crosses the tube axis, and the NO_2 planes must be tilted along the tube axis, to avoid steric repulsion between the two NO_2 groups. The other important factor is related to the distortion to the hexagonal carbon ring upon chemisorption of two NO_2 groups, as the two C atoms are pulled up. In **8**, the plucking up of two C atoms along the tube axis preserves a degree of local symmetry, while, in **12**, local symmetry is broken, resulting in more stresses to the tube structure. Both these factors contribute to the higher energy of **12** relative to **8**. The energy difference between the two ortho nitrite configurations, **13** and **17**, is due to similar reasons.

Overall, the adsorption of a second NO_2 group is energetically favored, especially for the ortho configurations **8** and **13**. As

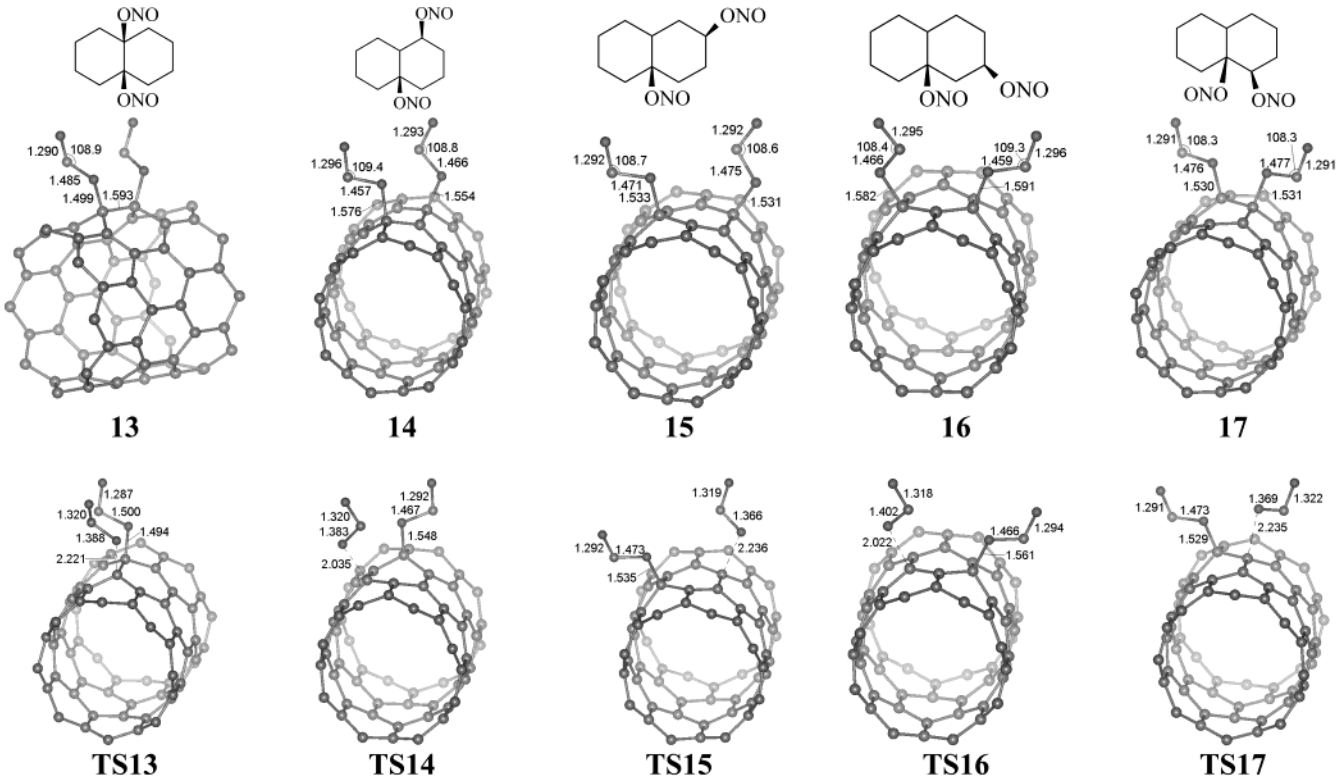

Figure 5. Optimized structures and transition structures for the adsorption of a second NO_2 on (8,0) single-walled carbon nanotube in the nitrite configuration. The distances shown are in angstroms.

TABLE 2: Energy Changes[a] and Barriers for the Adsorption of a Second NO_2 Group on an (8,0) Carbon Nanotube, with Energy in kilocalories per mole

	energy (GGA)			
structure	ΔE_{phys}	ΔE_{chem}	E_a (chemisorption barrier)	E_a (desorption barrier)
8	*b*	−15.3		15.3
9	−3.1	4.5	7.6[c]	
10	*b*	−11.6		11.6
12	−1.8	−3.8	0.3	2.4
13	−3.0	−21.4	4.2	22.6
14	−3.5	4.7	11.7	3.5
15	−4.1	−13.1	4.3	13.4
16	−3.8	5.0	10.6	1.8
17	−2.7	−7.1	8.4	12.8

[a] The energetics is defined in Figure 2. [b] There is no physisorption state in these two cases, as chemisorption takes place without an energy barrier. [c] In this case, the total energy increases monotonically from the physisorption to the chemisorption structure along the reaction path, and no transition state is identified. As a result, there is no desorption barrier, and the structure is unstable.

schematically shown in Figure 2, the implication is that desorption of NO_2 would be more difficult once two NO_2 groups are chemisorbed. This is especially true for the nitrite configuration **13**, for which the desorption barrier is 22.6 kcal/mol. Experimentally it was observed that complete recovery of a clean tube after NO_2 exposure took a long time (12 h),[19] which may indicate the presence of tubes with two chemisorbed NO_2 groups.

4. Adsorption and Desorption of N_2O_4. It is well-known that in the gas phase NO_2 is in an equilibrium with N_2O_4, which may also chemisorb on the nanotube surface. The doubly adsorbed structures discussed in the previous section may also desorb concertedly from the surface to form N_2O_4 directly.

The electronic structure of N_2O_4 has been studied in great detail by ab initio methods,[57−61] and its potential surface was carefully mapped out by McKee.[57] There are a number of isomers for N_2O_4, while here we limit ourselves to the most stable isomer, with the structure O_2N-NO_2.

The transition structures for a concerted desorption of two NO_2 groups to form N_2O_4 are shown in Figure 6. The most prominent feature is the fairly long distance between the two N atoms, just below 3.0 Å. This is in agreement with McKee's results on the transition structure for the formation of O_2N-NO_2 from two NO_2 groups with the N−N distance at 2.9 Å. In contrast, the experimental equilibrium N−N distance for N_2O_4 is 1.756 Å,[62] while the value obtained in our calculation is 1.830 Å. Also noticeable is the fact that the two C−N distances in **N17** differ by 0.7 Å, indicating a stepwise, rather than concerted, desorption of N_2O_4.

Listed in Table 3 are the barriers for N_2O_4 desorption from the six most stable configurations with two chemisorbed NO_2 groups. In all cases, the barrier is higher than that for the stepwise desorption as listed in Table 2. Such results are not surprising, since, in the desorption of N_2O_4, two C−N bonds are broken, while the N−N interaction is quite weak and provides little stabilization effects, due to the large N−N distance in the transition structures shown in Figure 6.

It should also be noted that the barriers for the reversal process, the direct adsorption of N_2O_4 to produce two chemisorbed NO_2 groups, is also quite high (Table 3). This is due to the fact that the N−N dissociation energy in N_2O_4 is 19.7 kcal/mol in our calculation, in good agreement with the previous reported value of 21.8 kcal/mol by a Gaussian-based DFT calculation using the Perdew−Wang functional,[58] although the experimental value is at 13.6 kcal/mol.[63] Thus, N_2O_4 plays a minor role in the overall equilibrium between adsorption and desorption.

5. Electronic Structure after NO_2 Adsorption. Chemisorption of NO_2 has a great effect on the electronic structure and conductivity of the (8,0) carbon nanotube. For the bare (8,0) tube, which is a semiconductor, our GGA calculation obtains a band gap of 0.62 eV, which is in very good agreement with the

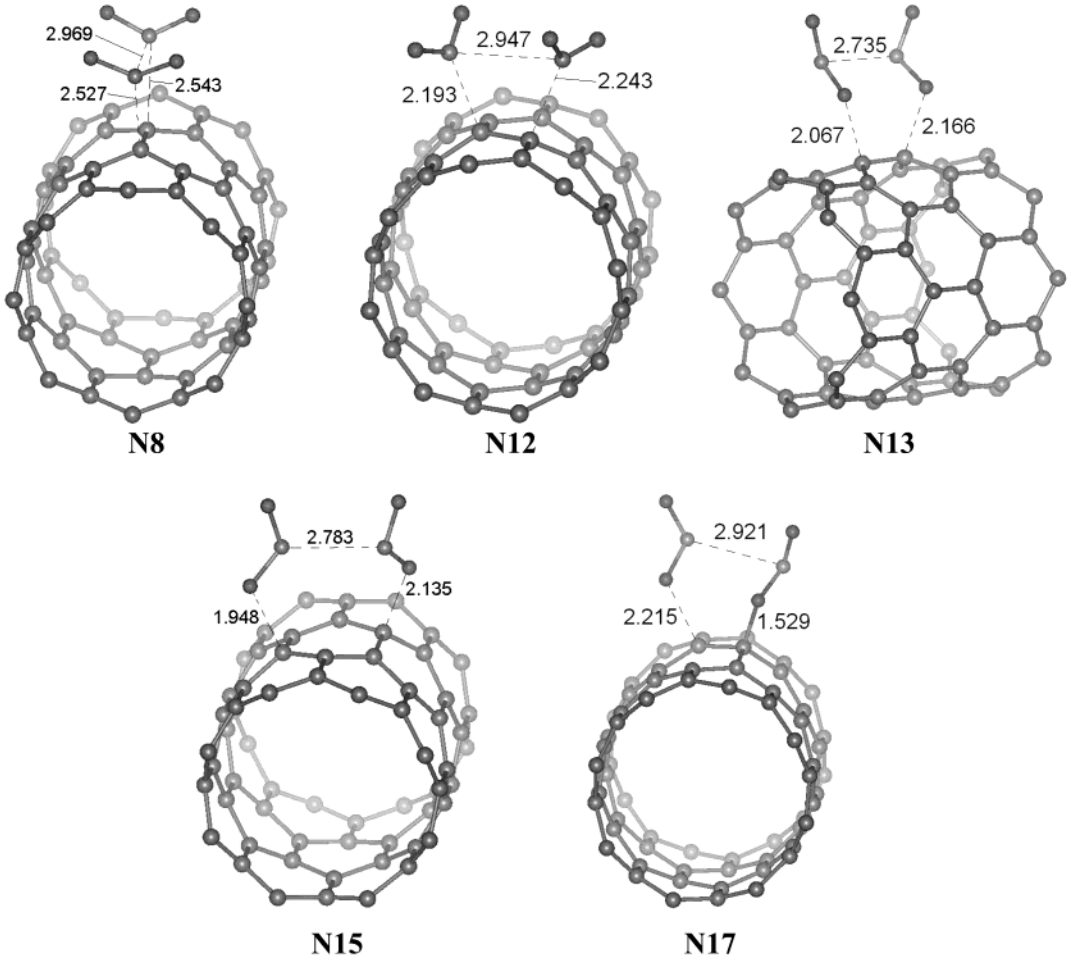

Figure 6. Transition structures for a concerted desorption of two NO_2 groups to form N_2O_4. The distances shown are in angstroms.

TABLE 3: Energy Changes and Barriers for N_2O_4 Adsorption on an (8,0) Tube with Energy in kilocalories per mole

	energy (GGA)			
structure	ΔE_{phys}[a]	ΔE_{chem}[a]	E_a[b] (chemisorption barrier)	E_a[b] (desorption barrier)
8	−1.2	5.9	23.2	16.2
10	−0.9	9.7	*c*	
12	−1.1	17.4	23.1	4.6
13	−1.8	−0.4	40.7	39.3
15	−1.8	7.9	33.6	23.9
17	−1.3	13.9	32.2	16.9

[a] Both physisorption and chemisorption energies are defined by $\Delta E = E$(adsorption structure) − E(bare tube) − E(free N_2O_4). [b] Activation barriers for chemisorption are relative to the corresponding physisorption states, while desorption barriers are relative to the chemisorption states. [c] We were unable to find a transition state for the desorption of N_2O_4 from **10**, probably because the two N atoms are well separated from each other in such a para configuration, making a concerted desorption of N_2O_4 unlikely.

previous LDA result of 0.6 eV.[13] The chemisorption of NO_2 changes the density of states (DOS), as shown in Figure 7 for the bare tube **1**, the singly adsorbed **2** and **4**, and the doubly adsorbed **8**, which are calculated with an expanded k-mesh.

As there is an unpaired electron on NO_2, the adsorption of one NO_2 means that the highest occupied band is now only half-filled. Correspondingly, there is a small DOS peak at the Fermi level for **2** and **4**, as shown in Figure 7b and c. The system thus becomes metallic, and a significant increase in conductivity is expected.

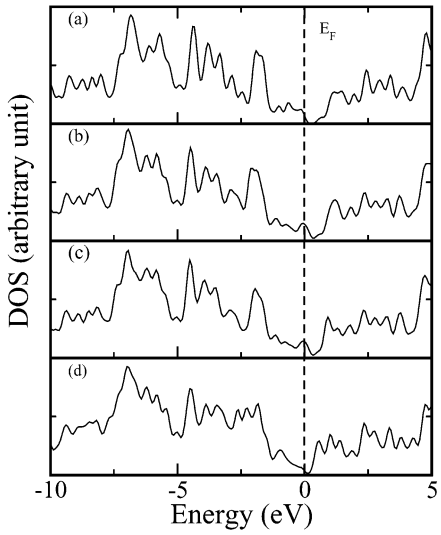

Figure 7. Density of states plots and the calculated band gaps for (a) **1**, a bare (8,0) tube; (b) **2**, singly adsorbed NO_2 in the nitro configuration; (c) **4**, singly adsorbed NO_2 in the nitrite configuration; and (d) **8**, doubly adsorbed NO_2 in the nitro configuration.

After chemisorption of two NO_2 groups, the system again becomes a semiconductor, with a drop of the DOS at the Fermi level, as exemplified by the plot for **8** in Figure 7d. Compared to the case of the bare tube, the band gap decreases to 0.38−0.45 eV (Table 4), which should also increase the conductivity. An increase in the conductivity of the carbon nanotubes was experimentally observed upon NO_2 exposure.[19] However, the

TABLE 4: Calculated Band Gaps for Singly and Doubly Adsorbed Structures

structure	band gap (eV)
(8,0) SWNT	0.62
2	
4	
8	0.38
10	0.45
13	0.44
15	0.45

diameter for the (8,0) tube used in our calculation is smaller than the typical tube diameter of 1−2 nm in experiments. As the reactivity is dependent on the curvature, it shall be worthwhile for future investigations to study the chemisorption of NO_2 on larger tubes and its effects on conductivity.

6. Summary. On the basis of DFT calculations, we find that, in terms of reactivity with NO_2, an (8,0) carbon nanotube is similar to an alkene, rather than a graphene, and a NO_2 group could easily adsorb on the nanotube exterior surface. The process is slightly endothermic and reversible with a small energy barrier. Furthermore, adsorption of a second NO_2 is energetically favorable. As a result, there is a significant barrier for the reversal process, the desorption of the second NO_2 group. Chemisorption of NO_2 also increases the conductivity of the (8,0) tube.

Acknowledgment. The work reported is supported by an Earmarked grant (Project No. CUHK 4252/01P) from the Research Grants Council of Hong Kong SAR Government. X.G.G. also acknowledges support from the NNSF of China, the Special Funds for Major State Basic Research of China, and the Key Projects of the Chinese Academy of Sciences. We are grateful for the generous allocation of computer time on the clusters of AlphaStations at the Chemistry Department, and the Center for Scientific Modeling and Computation, and on the high performance computing facilities at the Information Technology Service Center, all located at The Chinese University of Hong Kong.

Supporting Information Available: Atomic coordinates for all the stable and transition structures shown in the figures. This material is available free of charge via the Internet at http://pubs.acs.org.

References and Notes

(1) Iijima, S. *Nature (London)* **1991**, *354*, 56.
(2) Dresselhaus, M. S.; Dresselhaus, G. F.; Eklund, P. C. *Science of Fullerenes and Carbon Nanotubes*; Academic Press: New York, 1996.
(3) Dillon, A. C.; Jones, K. M.; Bekkedahl, T. A.; Kiang, C. H.; Bethune, D. S.; Heben, M. J. *Nature* **1997**, *386*, 377.
(4) Liu, C.; Fan, Y. Y.; Liu, M.; Cong, H. T.; Cheng, H. M.; Dresselhaus, M. S. *Science* **1999**, *286*, 1127.
(5) Ye, Y.; Ahn, C. C.; Witham, C.; Fultz, B.; Liu, J.; Rinzler, A. G.; Colbert, D.; Smith, K. A.; Smalley, R. E. *Appl. Phys. Lett.* **1999**, *74*, 2307.
(6) Wang, Q. Y.; Johnson, J. K. *J. Chem. Phys.* **1999**, *110*, 577.
(7) Simonyan, V. V.; Diep, P.; Johnson, J. K. *J. Chem. Phys.* **1999**, *111*, 9778.
(8) Schlapbach, L.; Zuttel, A. *Nature (London)* **2001**, *414*, 353.
(9) Chan, S. P.; Chen, G.; Gong, X. G.; Liu, Z. F. *Phys. Rev. Lett.* **2001**, *87*, 5502.
(10) Collins, P. G.; Bradley, K.; Ishigami, M.; Zettl, A. *Science* **2000**, *287*, 1801.
(11) Bradley, K.; Jhi, S. H.; Collins, P. G.; Hone, J.; Cohen, M. L.; Louie, S. G.; Zettl, A. *Phys. Rev. Lett.* **2000**, *85*, 4361.
(12) Zhu, X. Y.; Lee, S. M.; Lee, Y. H.; Frauenheim, T. *Phys. Rev. Lett.* **2000**, *85*, 2757.
(13) Jhi, S.-H.; Louie, S. G.; Cohen, M. L. *Phys. Rev. Lett.* **2000**, *85*, 1710.
(14) Sorescu, D. C.; Jordan, K. D.; Avouris, P. *J. Phys. Chem.* **2001**, *105*, 11227.
(15) Mann, D. J.; Hase, W. L. *Phys. Chem. Chem. Phys.* **2001**, *3*, 4376.
(16) Mawhinney, D. B.; Naumenko, V.; Kuznetsova, A.; Yates, J. T., Jr.; Liu, J.; Smalley, R. E. *J. Am. Chem. Soc.* **2000**, *122*, 2383.
(17) Kuznestova, A.; Popova, I.; Yates, J. T., Jr.; Bronikowski, M. J.; Huffman, C. B.; Liu, J.; Smalley, R. E.; Hwu, H. H.; Chen, J. G. *J. Am. Chem. Soc.* **2001**, *123*, 10699.
(18) Lu, X.; Zhang, L. L.; Xu, X.; Wang, N. Q.; Zhang, Q. E. *J. Phys. Chem. B* **2002**, *106*, 2136.
(19) Kong, J.; Franklin, N. R.; Zhou, C.; Chapline, M. G.; Peng, S.; Cho, K.; Dai, H. *Science* **2000**, *287*, 622.
(20) Peng, S.; Cho, K. J. *Nanotechnology* **2000**, *11*, 57.
(21) Chang, H. N.; Lee, J. D.; Lee, S. M.; Lee, Y. H. *App. Phys. Lett.* **2001**, *79*, 3863.
(22) Zhao, J. J.; Buldum, A.; Han, J.; Lu, J. P. *Nanotechnology* **2002**, *13*, 195.
(23) Cotton, F. A.; Wilkinson, G. *Advanced Inorganic Chemistry*, 3rd ed.; John Wiley & Sons: New York, 1972.
(24) Baldock, H.; Levy, N.; Scaife, C. W. *J. Chem. Soc.* **1949**, 2627.
(25) Brank, C. D.; Stevens, I. D. R. *J. Chem. Soc.* **1958**, 629.
(26) Schechter, H. *Rec. Chem. Prog.* **1964**, *25*, 55.
(27) Golding, P.; Powell, J. L.; Ridd, J. H. *J. Chem. Soc., Perkin Trans. 2* **1996**, 813.
(28) Pryor, W. A.; Lightsey, J. W.; Church, D. F. *J. Am. Chem. Soc.* **1982**, *104*, 6685.
(29) Giamalva, D. H.; Kenion, G. B.; Church, D. F.; Pryor, W. A. *J. Am. Chem. Soc.* **1987**, *109*, 7059.
(30) Sprung, J. L.; Akimoto, H.; Pitts, J. N. *J. Am. Chem. Soc.* **1971**, *93*, 4358.
(31) Akimoto, H.; Sprung, J. L.; Pitts, J. N. *J. Am. Chem. Soc.* **1972**, *94*, 4850.
(32) Sprung, J. L.; Akimoto, H.; Pitts, J. N. *J. Am. Chem. Soc.* **1974**, *96*, 6549.
(33) Sjövall, P.; So, S. K.; Kasemo, B.; Ranchy, R.; Ho, W. *Chem. Phys. Lett.* **1990**, *171*, 125.
(34) Moreh, R.; Finkelstein, Y.; Shechter, H. *Phys. Rev. B* **1996**, *53*, 16006.
(35) Cohen, M. L. *Phys. Rep.* **1984**, *110*, 293.
(36) Car, R.; Parrinello, M. *Phys. Rev. Lett.* **1985**, *55*, 2471.
(37) Remler, D. K.; Madden, P. A. *Mol. Phys.* **1990**, *70*, 921.
(38) Kresse, G.; Furthmüller, J. *Phys. Rev. B* **1996**, *54*, 11169.
(39) Kresse, G.; Hafner, J. *Phys. Rev. B* **1993**, *47*, 558.
(40) Kresse, G.; Hafner, J. *Phys. Rev. B* **1991**, *49*, 14251.
(41) Kresse, G.; Furthmüller, J. *Comput. Mater. Sci.* **1996**, *6*, 15.
(42) Tuckerman, M. E.; Ungar, P. J.; Vonrosenvinge, T.; Klein, M. L. *J. Phys. Chem.* **1996**, *100*, 12878.
(43) Marx, D.; Hutter, J. In *Modern methods and algorithms of quantum chemistry*; Grotendorst, J., Ed.; NIC Series; John von Neumann Institute for Computing: Jülich, 2000; Vol. 1, p 301.
(44) Perdew, J. P.; Zunger, A. *Phys. Rev. B* **1981**, *23*, 5048.
(45) Perdew, J. P. In *Electronic Structure of Solids '91*; Ziesche, P., Eschrig, H., Eds.; Academie Verlag: Berlin, 1991; p 11.
(46) Vanderbilt, D. *Phys. Rev. B* **1990**, *41*, 7892.
(47) Kresse, G.; Hafner, J. *J. Phys. Condens. Matter* **1994**, *6*, 8245.
(48) Kresse, G.; Hafner, J. *Phys. Rev. B* **1993**, *48*, 13115.
(49) Monkhorst, H. J.; Pack, J. D. *Phys. Rev. B* **1976**, *13*, 5188.
(50) Mills, G.; Jónsson, H.; Schenter, G. K. *Surf. Sci.* **1995**, *324*, 305.
(51) Jónsson, H.; Mills, G.; Jacobsen, K. W. In *Classical and Quantum Dynamics in Condensed Phase Simulations*; Berne, B. J., Ciccotti, G., Coker, D. F., Eds.; World Scientific: London, 1998; p 385.
(52) Jónsson, H. *Annu. Rev. Phys. Chem.* **2000**, *51*, 623.
(53) Henkelman, G.; Uberuaga, B.; Jónsson, H. *J. Chem. Phys.* **2000**, *113*, 9901.
(54) Henkelman, G.; Jónsson, H. *J. Chem. Phys.* **2000**, *113*, 9978.
(55) Morrison, R. T.; Boyd, R. N. *Organic Chemistry*, 6th ed.; Prentice Hall: Englewood Cliffs, NJ, 1992; p 568.
(56) McKee, M. L. *J. Phys. Chem.* **1989**, *93*, 7365.
(57) McKee, M. L. *J. Am. Chem. Soc.* **1995**, *117*, 1629.
(58) Stirling, A.; Pápai, I.; Mink, J.; Salahub, D. R. *J. Chem. Phys.* **1994**, *100*, 2910.
(59) Liu, R.; Zhou, X. *J. Phys. Chem.* **1993**, *97*, 4413.
(60) Bauschlicher, C. W., Jr.; Komornicki, A.; Roos, B. *J. Am. Chem. Soc.* **1983**, *105*, 745.
(61) Harcourt, R. D.; Skrezenek, F. L. *J. Phys. Chem.* **1990**, *94*, 7007.
(62) Domenech, J. L.; Andrews, A. M.; Belov, S. P.; Fraser, G. T.; Lafferty, W. J. *J. Chem. Phys.* **1994**, *100*, 6993.
(63) Vosper, A. J. *J. Chem. Soc.* **1970**, 625.